



Electrical properties of epoxy/ZnO nano-composite

Xinyu Wang¹ · Qingguo Chen¹ · Hongda Yang¹ · Kai Zhou¹ · Xin Ning¹

Received: 30 March 2018 / Accepted: 31 May 2018 / Published online: 5 June 2018
© Springer Science+Business Media, LLC, part of Springer Nature 2018

Abstract

The effects of nano-particles on the electrical properties of the epoxy/ZnO nano-composites are studied and the nonlinear conduction characteristics of the nano-composites are discussed. The morphology structure, relative permittivity, DC breakdown strength and DC conductivity of the nano-composites are measured. Micro-structure analysis shows that the ZnO nano-particles were well dispersed in the epoxy matrix. Experimental results show that the relative permittivity and DC conductivity of epoxy nano-composite with the filler loading of 0.5 wt% are lower than those of pure epoxy and the other nano-composites, but the 0.5 wt% has the highest breakdown strength among the epoxy/ZnO nano-composites. In addition, when the filler loading is larger than 0.5 wt%, the epoxy/ZnO nano-composite exhibits a distinct nonlinear conduction character, namely, that the DC conductivity is greatly dependent on the applied electric field. The variation of the electrical properties and the nonlinear conduction character against the filler loading may be attributed to the interaction zone around the nano-particles.

1 Introduction

Polymer materials play an important role in high voltage or high electric field due to the excellent electrical and mechanical properties, and have been widely used in electrical and electronic equipments [1]. However, space charges are easy to be formed in polymer materials and they would threaten the safe operation and reliability of electrical and electronic equipments [2–4]. In comparison with pure polymer materials and polymer micro-composites, polymer nano-composites present much more excellent electrical, mechanical and thermal properties [5]. These are attributed to the small size effect and the large specific surface area of nano-particles. By introducing nano-particles (such as, MgO, Al₂O₃, TiO₂ and ZnO) into the polymer materials, the conductivity, permittivity, breakdown strength and space charge formation can be improved [6–9]. For example, the addition of MgO nano-particles in low-density polyethylene (LDPE) can effectively suppress the space charge formation. Therefore, polymer nano-composites have got much more attention [6].

In addition, the nonlinear resistive field grading composite have been proved that it can also suppress the space charge accumulation by introducing a nonlinear conduction characteristic into the polymer materials [10]. This space charge suppression mechanism is different from that of nano-composites which suppress the space charge accumulation by deepening the trap energy [6–9]. The nonlinear resistive field grading composites were usually prepared by adding the SiC or ZnO micro-particles into the polymer materials [11–14]. This composites behave excellent insulating properties at a low electric field whereas present a high conductivity to dissipate the accumulated space charges at a high electric field. However, in order to achieve the nonlinear conduction characteristic, the filler loading of SiC or ZnO micro-particles is very high and is usually larger than 30 wt%. This would increase the processing difficulty and sharply decrease the mechanic properties of nonlinear resistive field grading composites. Compared with micro-particles, nano-particles can reduce the percolation threshold [15]. The percolation threshold for the resistivity of nano-composite takes place at much lower filler loading than that of micro-composite. The polymer nano-composites filling with ZnO nano-particles were investigated for their dielectric properties [16, 17]. The addition of ZnO nano-particles in epoxy resin shows lower permittivity values at lower filler loading over the frequency range of 10⁶–10⁹ Hz [18], but

✉ Xinyu Wang
13766866400@163.com

¹ Key Laboratory of Engineering Dielectrics and Its Application, Ministry of Education, Harbin University of Science and Technology, Harbin 150080, Heilongjiang, China

the nonlinear conduction characteristics of epoxy/ZnO nano-composites have rarely been reported.

In this paper, the epoxy resin, which is widely used in bushings, GIS/GIL spaces and printed circuit boards, is selected as the polymer matrix [19–21]. The aim of this work is to understand the effect of ZnO nano-particles on the permittivity, breakdown strength and the nonlinear conduction characteristics of epoxy nano-composites. The ZnO nano-particles are surface treated by silane coupling agent. The interaction zone around ZnO nano-particles plays an important role in the electrical properties of epoxy nano-composites. The nano-composites show better nonlinear conduction characteristics at higher filler loading and they can be potentially used to suppress the space charge accumulation and to regulate the electric field distribution.

2 Experiment sections

2.1 Materials

The pure epoxy resin was using bisphenol-A epoxy resin (PHOENIX WSR618 E-51) along with hardener (methylhexahydrophthalic anhydride, namely MHPA). The accelerator was 2, 4, 6-tris (dimethylaminomethyl) phenol (DMP-30). The weight ratio of epoxy resin to hardener and accelerator is 100:85:1. The nano-particles were commercially available ZnO made in China. The average particle size of nano-particles is 50 nm. Nano-particles were surface modified by silane coupling agent (KH560). The filler loadings were 0, 0.5, 1 and 3 wt%, respectively.

2.2 Preparation of epoxy nano-composites

Surface modification of ZnO nano-particles were carried out by silane coupling agent. The silane coupling agent was dissolved in a mixture of distilled water and anhydrous ethanol at room temperature and was ultrasonic mixing for 10 min. The ZnO nano-particles were then filled into the solution containing silane coupling agent and were ultrasonic mixing for 1 h again. The modified ZnO nano-particles were then obtained after drying and grinding.

Epoxy resin and hardener were dried at 60 °C to remove moisture before preparing the epoxy nano-composites. The modified ZnO nanoparticles were added into epoxy resin and were high-speed shearing at 60 °C for 10 min. The hardener and accelerator were then added into the mixture of epoxy resin and were electrically blending at 60 °C for 30 min. The mixture was vacuum degassing to remove the air bubbles and was subsequently casted into the mould. The nano-composites were cured by three steps. They were pre-cured at 80 °C for 2 h, then cured at 100 °C for 2 h, and post-cured

at 120 °C for 6 h. The average thickness of the samples was about 0.3 mm.

2.3 Characterization

The morphology of epoxy nano-composites was observed using scanning electron microscopic (SEM) at acceleration voltage of 5 kV. The flat section of specimens was prepared and was then sputter coated with gold.

Relative permittivity was measured at 25 °C using broadband dielectric spectrometer (Concept 80). The applied frequency was in the range of 0.1–10⁶ Hz. The applied voltage was 1 V. Both sides of specimens were coated with gold. The gold electrode was 30 mm in diameter.

Breakdown strength was evaluated by a sphere–sphere electrode system. The DC voltage was raised from 0 kV at a rate of 1 kV/s until the specimen got punctured. The sphere electrode was 25 mm in diameter. The entire electrode system was immersed in the transformer oil to avoid surface flashover. A set of 10 specimens for each filler loading were tested and were used to calculate the breakdown strength.

DC conductivity measurement was carried out with a three-electrode system and a picoammeter of EST122 which was made in China. The measuring electrode was 50 mm in diameter. The gap distance between the measuring electrode and the grounding electrode is 2 mm. The DC current density was measured after applying a DC electric field for 30 min and was then used to calculate the DC conductivity. The applied electric field was ranged from 3 to 36 kV/mm.

3 Results and discussion

3.1 Nano-particle dispersion characterization

Figure 1 shows the SEM images of pure epoxy and epoxy/ZnO nano-composites. An uneven section can be observed in the SEM image of pure epoxy as shown in Fig. 1a. By contrast, as shown in Fig. 1b, the ZnO nano-particles with the filler loading of 3 wt% are well dispersed in the epoxy matrix, and only a few large agglomerates can be observed. This indicates that the preparation used in this work can prevent the nano-particles agglomeration.

3.2 Relative permittivity

The relationships between the relative permittivity and the applied frequency for pure epoxy and epoxy/ZnO nano-composites are shown in Fig. 2a. The relative permittivity of epoxy nano-composites with different filler loadings at a constant temperature is decreased with the increasing frequency. The variation of the relative permittivity against the applied frequency is mainly attributed to the

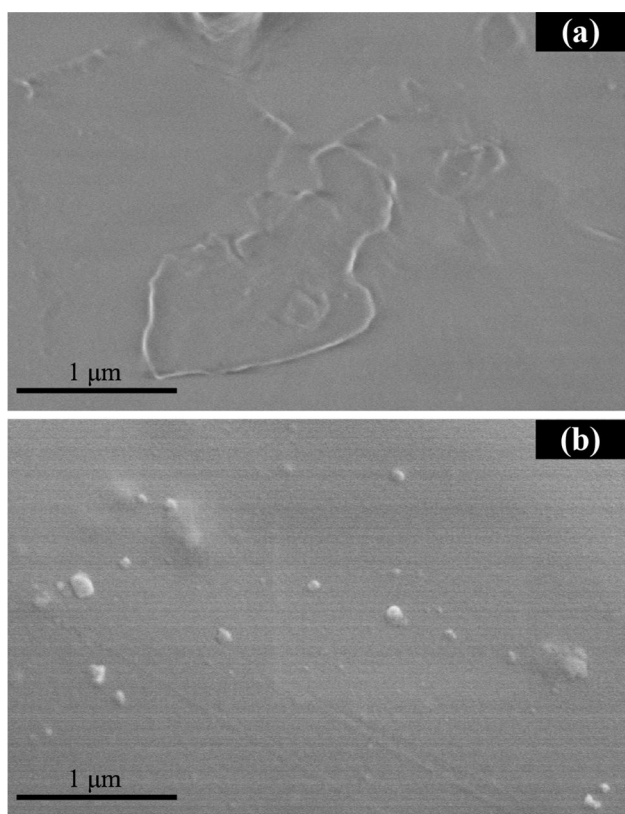


Fig. 1 SEM images of a pure epoxy (a) and 3 wt % epoxy/ZnO nanocomposites (b)

polarization associated with epoxy matrix as well as nanoparticles and the interface polarization at the matrix-particle interface [22]. The polarization of epoxy matrix is usually associated with the number of orientable dipolar functional groups in the epoxy chain and the ability of these orientable dipoles to orient under the applied electric field. Under lower applied frequency, nearly all of orientable dipoles can orient along the direction of the applied electric field, and these orientable dipoles contribute to the polarization, so the relative permittivity at the lower applied frequency is much larger. The number of the orientable dipoles orienting along the direction of the applied electric field becomes to reduce gradually with the increasing applied frequency, resulting in the continuous decrease in the relative permittivity. Under very high applied frequency, only a few orientable dipoles can orient along the direction of the applied electric field, so the relative permittivity is very small at this frequency. The inherent polarization of nanoparticles and the interface polarization at the matrix-particle interface against the applied frequency behave similar tendencies with that of epoxy matrix. Thus, these combined effects lead to the decrease of the relative permittivity with the increasing frequency.

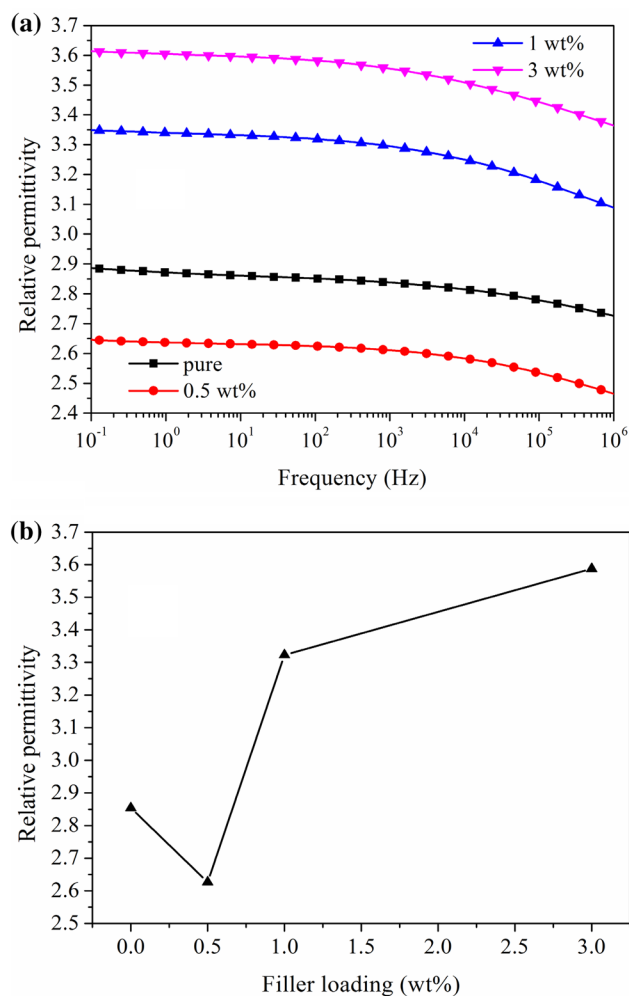


Fig. 2 Relative permittivity of specimens, relationship between the relative permittivity and the applied frequency (a), relationship between the relative permittivity and the filler loading at 50 Hz (b)

Figure 2b shows the relationship between the relative permittivity and the filler loading at 50 Hz. The relative permittivity is decreased when the filler loading is increased from 0 to 0.5 wt%, whereas it begins to be increased when the filler loading is larger than 0.5 wt%. Similar observations have been reported for polymer based nano-composites [23, 24]. This may be attributed to the effect of the interaction zone between the polymer matrix and the nanoparticles. The interaction zone is a low density region as well as a less stoichiometric region. According to the multi-region structure model consisting of a bonded region, a transition region and a normal region [25, 26], the nanoparticles at the slight filler loading can be regarded as isolated particles. The movement of orientable dipoles along the direction of electric field can be restricted by the interaction zone, resulting in the decrease of relative permittivity. By contrast, the distance between neighboring nanoparticles becomes gradually short with the increasing filler loading,

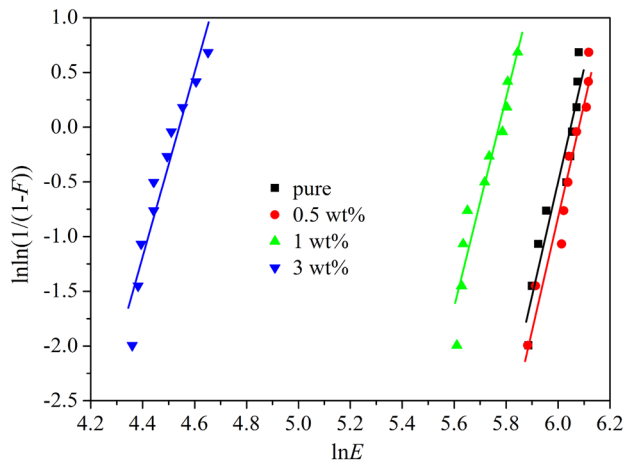


Fig. 3 Weibull curves of the breakdown strength of the nano-composites with different filler loadings

Table 1 Weibull parameters of different specimens

Specimens	0 wt%	0.5 wt%	1 wt%	3 wt%
α (kV/mm)	423.4	437.1	321.3	93.8
β	10.5	10.2	9.5	8.3

or even the transition regions of neighboring nano-particles may overlap. And then the nano-particles begin to play an important role in the electrical properties of polymer based nano-composites. As the relative permittivity of nano-particles is usually much larger than that of polymer matrix, the relative permittivity of nano-composite with a higher filler loading is much larger.

3.3 Breakdown strength

Two-parameter Weibull distribution is used to evaluate the breakdown behavior of epoxy/ZnO nano-composites with different filler loading, as shown in Fig. 3, and the Weibull distribution function can be described as below,

$$F = 1 - \exp \left[- \left(E_b / \alpha \right)^\beta \right] \quad (1)$$

where F is the cumulative probability of breakdown strength. E_b is the measured values of breakdown strength. α is the scale parameter known as the Weibull breakdown strength (EBD) which is the electric field when the cumulative probability of breakdown strength is 63.2%. β is the shape parameter which characterizes the scatter of breakdown strength. The Weibull parameters (namely, α and β) for each specimen are shown in Table 1.

It is observed from Fig. 3 and the scale parameters (α) given as in Table 1 that the breakdown strength increases for 0.5 wt% filler loading, whereas it decreases with an

increase in the filler loading up to 3 wt%. Our observations are nearly consistent with that reports on the breakdown strength of polymer based nano-composites. Tian finds that the addition of 0.1 wt% ZnO nano-particles in LDPE exhibits much more excellent breakdown performance than LDPE and other nano-composites with higher filler loadings [9]. Similar observations also have been found in epoxy nano-composites [26]. The short-time electrical breakdown is mainly related to the density of free carriers and the mobility in the electric field [7]. When the nano-particles are added into the polymer matrix, the interaction zone around nano-particles is then formed and may introduce the deep trap sites at the matrix-particle interface. Based on the multi-region structure model [25, 26], the nano-particles in the nano-composite with slight filler loading can be treated as isolated particles. The free carriers can be captured by these deep trap sites and are unlikely to transport, resulting in the decrease in the density of free carriers. In addition, the thickness of the interaction zone (especially, the transition region) is usually shorter than the mean free path [26], the free carriers may lose their energy obtained from the electric field due to the collision with defects in the interaction zone, and their mobility is then reduced. The reduction of free carrier density and mobility at the slight filler loading contributes to the increase in the breakdown strength. With the increasing filler loading, the interaction zone (especially, the transition regions) may overlap, leading to an increase in the thickness of the transition region. When the mean free path is less than the thickness of the transition region, carriers can gain much more energy from the electric field to transport, leading to an increase in the free carrier density and mobility. As a result, the electrical breakdown strength decreases at higher filler loading.

3.4 DC conductivity and nonlinear conduction characteristics

Figure 4a illustrates the conductivity with respect to the filler loading at the applied electric field of 15 kV/mm. It can be clearly seen that the conductivity decreases when the filler loading is up to 0.5 wt% and then increases when the filler loading is larger than 0.5 wt%. As is known, the conductivity is proportional to the free carrier density and mobility. Based on the multi-region structure model [25, 26], the decreasing free carrier density and mobility at the slight filler loading contribute to the reduction of the conductivity. With the increasing filler loading, the free carrier density and mobility will increase and result in an increase in the conductivity.

The relationship between the conductivity and the applied electric field is shown in Fig. 4b. The conductivity of the 0 and 0.5 wt% is very weakly dependent on the electric field. A similar tendency can be seen in the 1 and 3 wt% when the applied electric field is up to 15 kV/mm. By contrast, when

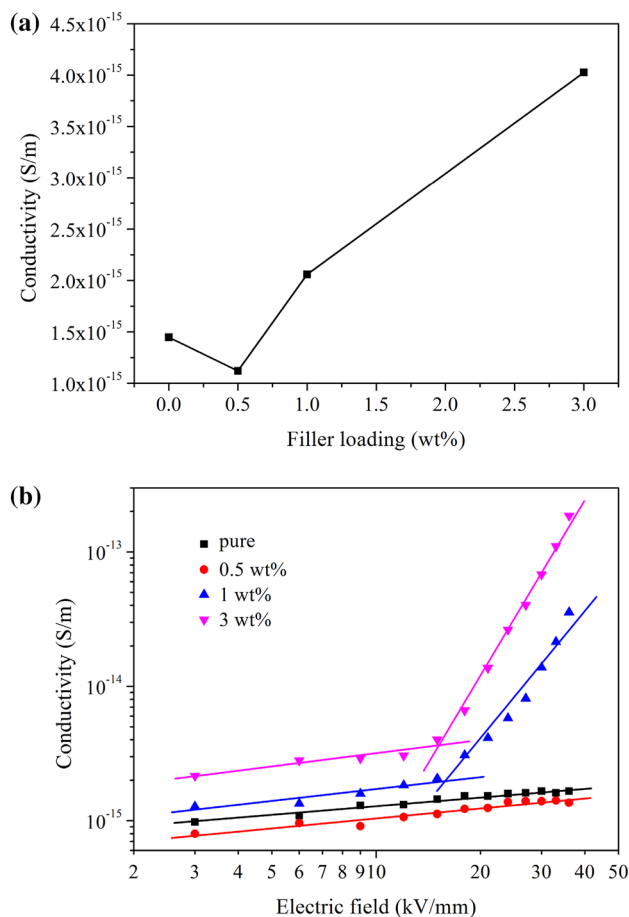


Fig. 4 Conductivity of different specimens at 15 kV/mm (a), and relationship between the conductivity and electric field (b)

the applied electric field is greater than 15 kV/mm, the conductivity of the 1 and 3 wt% shows a great dependence on the electric field and increases quickly with the increasing electric field. These results indicate that the 1 and 3 wt% behave distinct nonlinear conduction characteristics.

To evaluate the nonlinear conduction characteristic, the conductivity (γ) is usually described as a function of the applied electric field, as follows [13],

$$\gamma = \gamma_0 (E/E_0)^{\alpha_n} \quad (2)$$

where γ_0 is the switching conductivity, E is the applied electric field, E_0 is the switching electric field, and α_n is the nonlinearity exponent.

Table 2 exhibits the nonlinearity exponent (α_n) of each specimen. Both of the 0 and 0.5 wt% present very weak nonlinear conduction characteristics in the whole of applied electric field. In comparison, the 1 wt% behaves a stronger nonlinear conduction characteristic in the high electric field, and the nonlinearity exponent is 3.17. When the filler loading is 3 wt%, it is 4.41. Thus, the nonlinear conduction

Table 2 Nonlinearity exponent of different specimens

Specimens	0 wt%	0.5 wt%	1 wt%	3 wt%
High field	0.22	0.24	3.17	4.41
Low field	0.22	0.24	0.29	0.33

characteristic is closely related to the filler loading of nanoparticles. According to the multi-region structure model [25, 26], the deep trap sites are introduced in interaction zone at the slight filler loading. The carriers captured by these deep trap sites cannot get out until they obtain enough energy from very high electric field. The free carrier density is very few and the mobility is very slow, resulting in a weak dependence on the electric field. By comparison, with the increasing filler loading, the migration distance of free carriers increases as the thickness of the interaction zone is larger than the mean free path. The carriers can be easy to gain energy from the electric field and are rarely restrained by the traps in the interaction zone, resulting in the enhancement of the carrier mobility. A higher mobility contributes to a larger nonlinearity exponent.

4 Conclusions

Epoxy/ZnO nano-composites have been investigated. The relative permittivity decreases when the filler loading is increased from 0 to 0.5 wt%, whereas it increases when the filler loading is increased from 0.5 to 3 wt%. A similar observation can be found in the relationship between the DC conductivity and the filler loading. In contrast, the DC breakdown strength has the maximum value at the filler loading of 0.5 wt%, compared with the 0, 1 and 3 wt%. Furthermore, both of the 1 and 3 wt% show great nonlinear conduction characteristics, which may be potential to suppress the space charge accumulation. The results indicate that the interaction zone around ZnO nano-particles plays an important role in the relative permittivity, breakdown strength, DC conductivity and nonlinear conduction characteristics. More researches on the nonlinear conduction characteristics and their mechanism as well as application of epoxy/ZnO nano-composites will be continued to study.

Acknowledgements This work was supported by the National Science Foundation of China (Nos. 51677046, 51407051).

References

- V.A. Zakrevskii, N.T. Sudar, A. Zaopo, Y.A. Dubitsky, Mechanism of electrical degradation and breakdown of insulating polymers. *J. Appl. Phys.* **93**, 2135–2140 (2003)

2. J.M. Yang, X. Wang, H. Zhao, W.L. Zhang, M.Z. Xu, Influence of moisture absorption on the DC conduction and space charge property of MgO/LDPE nanocomposite. *IEEE Trans. Dielectr. Electr. Insul.* **21**, 1957–1964 (2014)
3. H. Hama, T. Hikosaka, S. Okabe, H. Okubo, Cross-equipment study on charging phenomena of solid insulators in high voltage equipment. *IEEE Trans. Dielectr. Electr. Insul.* **14**, 508–519 (2007)
4. D.-E.A. Mansour, H. Kojima, N. Hayakawa, F. Endo, H. Okubo, Surface charge accumulation and partial discharge activity for small gaps of electrode/epoxy interface. *IEEE Trans. Dielectr. Electr. Insul.* **16**, 1150–1157 (2009)
5. T. Tanaka, G.C. Montanari, R. Mulhaupt, Polymer nanocomposites as dielectrics and electrical insulation—perspectives for processing technologies, material characterization and future applications. *IEEE Trans. Dielectr. Electr. Insul.* **11**, 763–784 (2004)
6. T. Takada, Y. Hayase, Y. Tanaka, T. Okamoto, Space charge trapping in electrical potential well caused by permanent and induced dipoles for LDPE/MgO nanocomposite. *IEEE Trans. Dielectr. Electr. Insul.* **15**, 152–160 (2008)
7. B.Y. Zhang, W.Q. Gao, P.F. Chu, Z. Zhang, G.X. Zhang, Trap-modulated carrier transport tailors the dielectric properties of alumina/epoxy nanocomposites. *J. Mater. Sci. Mater. Electron.* **29**, 1964–1974 (2018)
8. B.X. Du, J.W. Zhang, Y. Gao, Effects of TiO₂ particles on surface charge of epoxy nanocomposites. *IEEE Trans. Dielectr. Electr. Insul.* **19**, 755–762 (2012)
9. F.Q. Tian, Q.Q. Lei, X. Wang, Y. Wang, Investigation of electrical properties of LDPE/ZnO nanocomposite dielectrics. *IEEE Trans. Dielectr. Electr. Insul.* **19**, 763–769 (2012)
10. K. Tavernier, B.R. Varlow, D.W. Auckland, M. Ugur, Improvement in electrical insulators by nonlinear fillers. *IEEE Proc. Sci. Meas. Technol.* **146**, 88–94 (1999)
11. K.P. Donnelly, B.R. Varlow, Nonlinear dc and ac conductivity in electrically insulating composites. *IEEE Trans. Dielectr. Electr. Insul.* **10**, 610–614 (2003)
12. X. Wang, J.K. Nelson, L.S. Schadler, H. Hillborg, Mechanisms leading to nonlinear electrical response of a nano p-SiC/silicone rubber composite. *IEEE Trans. Dielectr. Electr. Insul.* **17**, 1687–1696 (2010)
13. T. Christen, L. Donzel, F. Greuter, Nonlinear resistive electric field grading part 1: theory and simulation. *IEEE Electr. Insul. Mag.* **26**, 47–59 (2011)
14. S.M. Lebedev, O.S. Gefle, A.E. Strizhkov, Novel polymeric composites with nonlinear current-voltage characteristic. *IEEE Trans. Dielectr. Electr. Insul.* **20**, 289–295 (2013)
15. J.I. Hong, L.S. Schadler, R.W. Siegel, E. Martensson, Rescaled electrical properties of ZnO/low density polyethylene nanocomposites. *Appl. Phys. Lett.* **82**, 1956–1958 (2003)
16. J.I. Hong, P. Winberg, L.S. Schadler, R.W. Siegel, Dielectric properties of zinc oxide/low density polyethylene nanocomposites. *Mater. Lett.* **59**, 473–476 (2005)
17. S.C. Tjong, G.D. Liang, Electrical properties of low density polyethylene/ZnO nanocomposites. *Mater. Chem. Phys.* **100**, 1–5 (2006)
18. S. Singha, M.J. Thomas, Influence of filler loading on dielectric properties of epoxy-ZnO nanocomposites. *IEEE Trans. Dielectr. Electr. Insul.* **16**, 531–542 (2009)
19. N.S. Jyothi, T.S. Ramu, M. Mandlik, Temperature distribution in resin impregnated paper insulation for transformer bushings. *IEEE Trans. Dielectr. Electr. Insul.* **17**, 931–938 (2010)
20. D.-E.A. Mansour, H. Kojima, N. Hayakawa, F. Endo, H. Okubo, Partial discharges and associated mechanisms for micro gap delamination at epoxy spacer in GIS. *IEEE Trans. Dielectr. Electr. Insul.* **17**, 855–861 (2010)
21. K. Fukunaga, T. Maeno, K. Okamoto, Three-dimensional space charge observation of ion migration in a metal-base printed circuit board. *IEEE Trans. Dielectr. Electr. Insul.* **10**, 458–462 (2003)
22. S. Singha, M.J. Thomas, Dielectric properties of epoxy nanocomposites. *IEEE Trans. Dielectr. Electr. Insul.* **15**, 12–23 (2008)
23. M. Roy, J.K. Nelson, R.K. MacCrone, L.S. Schadler, C.W. Reed, R. Keefe, W. Zenger, Polymer nanocomposite dielectrics—the role of the interface. *IEEE Trans. Dielectr. Electr. Insul.* **12**, 629–643 (2005)
24. Y.S. Han, S.T. Li, D.M. Min, Nonlinear conduction and surface potential decay of epoxy/SiC nanocomposites. *IEEE Trans. Dielectr. Electr. Insul.* **24**, 3154–3164 (2017)
25. S.T. Li, G.L. Yin, G. Chen, J.Y. Li, S.N. Bai, L.S. Zhong, Y.X. Zhang, Q.Q. Lei, Short-term breakdown and long-term failure in nanodielectrics: a review. *IEEE Trans. Dielectr. Electr. Insul.* **17**, 1523–1535 (2010)
26. S.T. Li, G.L. Yin, S. Bai, J.Y. Li, A new potential barrier model in epoxy resin nanodielectrics. *IEEE Trans. Dielectr. Electr. Insul.* **18**, 1535–1543 (2011)